Analysis of Excitation Functions in Cm(C,xn)No Reactions*

TORBJORN SIKKELAND, ALBERT GHIORSO, AND MATTI J. NURMIA
Lawrence Radiation Laboratory, University of California, Berkeley, California 94720
(Received 8 April 1968)

Excitation functions for the synthesis of ^{251}No, ^{252}No, ^{253}No, ^{254}No, ^{255}No, ^{256}No, and ^{257}No in the bombardments of ^{244}Cm, ^{246}Cm, and ^{248}Cm with ^{12}C and ^{13}C are presented. A good fit to these functions has been obtained by the use of the Jackson formula as modified to include fission and angular-momentum effects. Experimental values of $\langle\Gamma_n/\Gamma_f\rangle_{av}$ are compared with the semiempirical formula of Fujimoto and Yamaguchi and the following new empirical formula: $\log_{10}(\Gamma_n/\Gamma_f)=-0.276Z+f(N)$, where $f(N)$ is $5.46+0.140N$ for $N\leqq153$ and $19.23+0.050N$ for $N\geqq153$. A brief discussion of Γ_n/Γ_f systematics of transberkelium nuclides and the effect of the 152-neutron subshell is given.

I. INTRODUCTION

HEAVY-ION reactions, characterized by the formation of a compound nucleus followed by neutron emission, constitute an efficient method for the production of neutron-deficient nuclides. In many cases the identification of the products is based on the analysis of their excitation functions. In regions where fission can be ignored, the use of Jackson's neutron-emission formula,[1] as modified to include angular-momentum effects, has been successful in fitting the experimental functions.[2]

In the heavy-element region, fission competes strongly with neutron emission in the decay of the compound nucleus, and the cross sections depend critically on the value of the ratio Γ_n/Γ_f, where Γ_n and Γ_f are the partial widths for neutron emission and fission, respectively. This ratio varies both with Z and A and a knowledge of its systematic behavior is therefore of great importance in the synthesis of the heaviest nuclides. Vandenbosch and Huizenga have made an extensive survey of experimental Γ_n/Γ_f values obtained in γ-, n-, p-, d-, and α-induced reactions.[3] They find such values for Pu isotopes to be fairly well reproduced by the formula of Fujimoto and Yamaguchi.[4]

Up to now, nuclides of californium have been the heaviest ones for which an extensive set of production-cross-section data in heavy-ion–induced reactions has been obtained and analyzed.[5] Again the formulas by Jackson and by Fujimoto and Yamaguchi were successfully applied.

Recently, nuclides of element 102, nobelium, with mass numbers from 251 to 257, have been produced in Cm(C,xn)No reactions.[6] In the present paper we shall analyze the excitation functions obtained in that work. In these reactions, nuclides with neutron numbers in excess of the $N=152$ neutron subshell are produced, and it will be of special interest to observe the effect of that shell on the value of the ratio Γ_n/Γ_f.

II. EXPERIMENTAL

We shall give only a brief account of the experimental arrangement since a more detailed description has been reported elsewhere.[6] The essentially monoisotopic targets of ^{244}Cm, ^{246}Cm, and ^{248}Cm were made by molecular deposition to a thickness of between 0.2 and 0.5 mg/cm^2 on about 5 mg/cm^2 beryllium metal. Beams of 10.4-MeV/nucleon ^{12}C and ^{13}C ions from the Berkeley Hilac were degraded to the desired energies by the use of Be foils. The energy spectrum of the ions leaving the target was occasionally measured by the use of a diffused-junction Si detector. The most probable energy is believed to be accurate to ±2 MeV. The beam currents were typically 2×10^{12} particles/sec in an area of 0.2 cm^2. Atoms recoiling from the target are stopped in a stream of helium at 600 Torr and carried by this gas through an orifice about 0.2 mm in diameter into an evacuated space. The gas jet impinges a few millimeters away on the periphery of a wheel and a large fraction ($\sim$80%) of the heavy atoms attach themselves to its surface. At regular intervals the wheel is digitally rotated about 50° to expose the collected atoms to Au-Si surface-barrier α-particle detectors. In this series of experiments four detectors, equally spaced along the circumference of the wheel, were used simultaneously in order to obtain half-life information as well as α-particle energies. Spontaneous fissions were also recorded in these experiments.

The total counting efficiency, defined as the ratio of the counts observed to the α disintegrations undergone by the nuclei transmuted from the target, was found experimentally to be about 10%. Half-lives and yield of spontaneous fission activities were also measured in separate experiments in which the recoils were caught on a rotating drum in vacuum and the fission fragments were recorded by mica detectors placed along the periphery of the drum.

* This work was done under the auspices of the U. S. Atomic Energy Commission.

[1] J. D. Jackson, Can. J. Phys. **34**, 767 (1956).
[2] T. Sikkeland, Arkiv Fysik **36**, 539 (1967).
[3] R. Vandenbosch and J. R. Huizenga, in *Proceedings of the Second United Nations International Conference on the Peaceful Uses of Atomic Energy, 1958* (United Nations, New York, 1958), Vol. 15, p. 688.
[4] Y. Fujimoto and Y. Yamaguchi, Progr. Theoret. Phys. (Kyoto) **5**, 76 (1950).
[5] T. Sikkeland, J. Maly, and D. F. Lebeck, Phys. Rev. **169**, 1000 (1968).
[6] A. Ghiorso, T. Sikkeland, and M. J. Nurmia, Phys. Rev. Letters **18**, 401 (1967).

III. EXPERIMENTAL RESULTS

α energy spectra obtained in these experiments have been given previously.[6] A summary of the decay characteristics of the No isotopes is given in Table I. Only about 80 events were recorded in the decay of ^{251}No, whereas for the other ones several hundred events were used in the half-life measurements. In the estimation of the cross sections we assumed the α branching to be 100% for all isotopes except for ^{252}No.

In the analysis of the α spectra, a difficulty was encountered by the discovery that the 2.6-sec, 7.14-MeV ^{214}Ra decayed by electron capture with a branching of $(9.5\pm0.8)\times10^{-4}$ to the 4-msec, 8.43-MeV ^{214}Fr. The isotope ^{214}Ra is produced from lead impurities in the targets, and in our experimental arrangement this results in an apparent 2.6-sec, 8.4-MeV α activity that in some instances interfered with the radiations from ^{252}No and ^{256}No (see Table I). However, the number of α particles from ^{214}Fr present in the observed peak at 8.4 MeV could be computed from the observed number of α particles from ^{214}Ra and its electron capture branching. Thus, corrected half-lives and cross sections for these two No isotopes could be obtained. The extent of such corrections in cross-section measurements is illustrated in Fig. 1 for the systems (^{244}Cm+^{12}C), (^{248}Cm +^{12}C), and (^{248}Cm+^{13}C). Here the measured ratio (yield of 8.4-MeV α)/(yield of 7.14-MeV α) is plotted versus ion energy. For comparison the same plot for the system (Pb^{nat}+^{12}C) has also been included. We see that, for the latter system, the ratio is independent of ion energy, suggesting that the 8.4-MeV α particles are coming from a daughter of the 2.6-sec, 7.14-MeV ^{214}Ra. For the other systems the 8.4-MeV α particles are mostly those from ^{214}Fr, whereas at lower energy the ratio is substantially higher than that for Pb. The half-lives of ^{252}No and ^{256}No were measured at the lowest energies, where the correction due to ^{214}Fr was small.

The cross sections for the production of the various No isotopes are plotted versus ion energy in Figs. 2–7. To compare the cross sections for the production of the 2.5-sec spontaneous-fission (SF) emitter with those of the 2.5-sec, 8.4-MeV α emitter, the former have been multiplied by 2. The curves represent calculated values as described later in Sec. IV. Typical errors are indicated by error bars and are based on counting statistics only. In addition to these errors we have uncertainties and inhomogeneities in the target thicknesses and a variation and systematic errors in the collection efficiency which together might be as high as 50%.

TABLE I. Decay properties of various isotopes of element 102.

Isotopes	Half-life (sec)	E_α(MeV) ±0.02	SF/α ratio[a]
^{251}102	0.8±0.3	8.60(80%) 8.68(20%)	
^{252}102	2.5±0.3	8.41	½
^{253}102	105±15	8.01	
^{254}102	55±5	8.10	
^{255}102	185±15	8.11	
^{256}102	2.8±0.3	8.43	
^{257}102	23±3	8.23(50%) 8.27(50%)	

[a] SF =spontaneous fission.

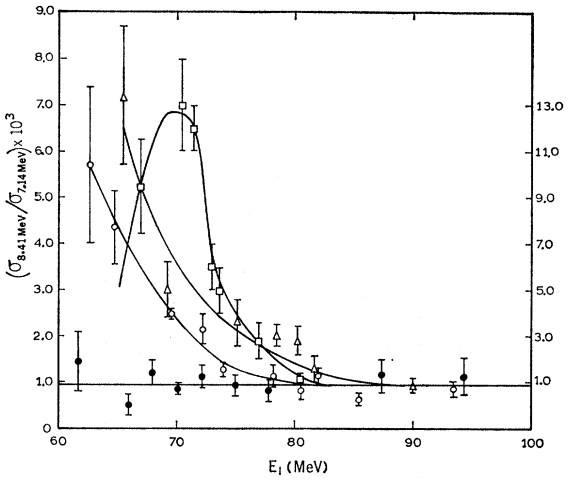

FIG. 1. Ratio between the yield of 8.4-MeV α to that of 7.14-MeV α in units of 10^{-3} measured as a function of ion energy for the systems Pb^{nat}+C (●); ^{244}Cm+^{12}C (△); ^{248}Cm+^{12}C (○); and ^{248}Cm+^{13}C (□). The ordinate scale on the left is for the first three systems and that on the right is for ^{248}Cm+^{13}C.

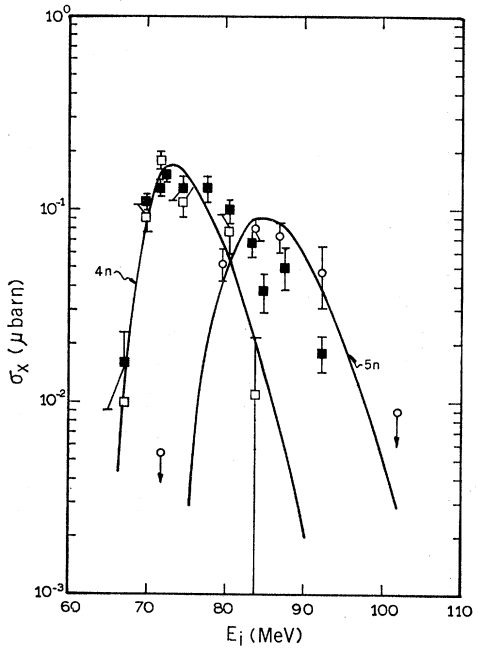

FIG. 2. Experimental cross sections plotted versus ion energy for ^{244}Cm(^{12}C,xn)$^{256-x}$No reactions. The open squares, solid squares, and circles correspond to $x=4$ (α emitter), $x=4$ (SF emitter), and $x=5$, respectively. The yields of the SF emitter have been multiplied by 2. The curves represent the function $\sigma_{CN}P_x$ normalized at the peak to the experimental points. The energy scales for the curves are displaced ΔE MeV relative to that of the points. Values for ΔE are given in Table II.

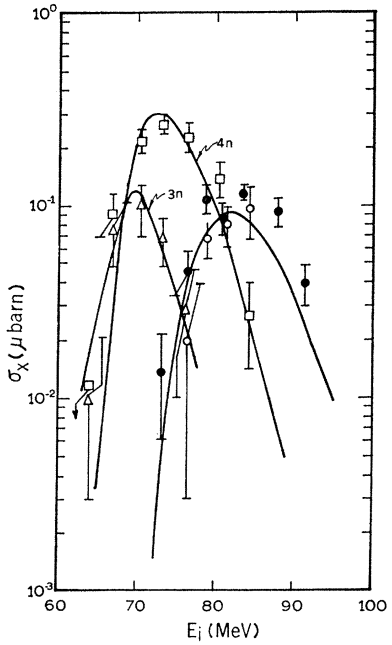

FIG. 3. Experimental cross sections plotted versus ion energy for ^{244}Cm(^{13}C,xn)$^{257-x}$No reactions. The triangles, squares, open circles, and closed circles correspond to $x=3$, $x=4$, $x=5$ (α emitter), and $x=5$ (SF emitter), respectively. The yields of the SF emitter have been multiplied by 2. The curves represent the function $\sigma_{CN}P_x$ normalized as explained in the caption to Fig. 2.

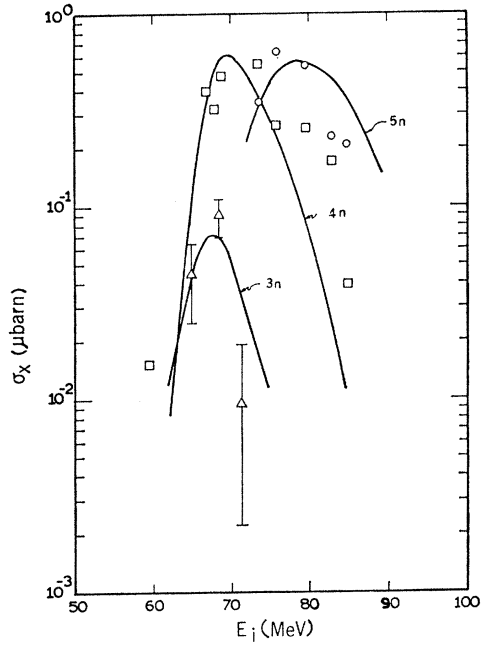

FIG. 5. Experimental cross sections plotted versus ion energy for ^{246}Cm(^{13}C,xn)$^{259-x}$No. The triangles, squares, and circles correspond to $x=3$, $x=4$, and $x=5$, respectively. The curves represent the function $\sigma_{CN}P_x$ normalized as explained in the caption to Fig. 2.

No errors are given for the systems ^{246}Cm(^{13}C,4n)-^{255}No and ^{246}Cm(^{13}C,5n)^{254}No (see Fig. 5) because of the near coincidence of the α energies of these two No isotopes. Consequently, their yield measurements had to be based on the separation of a decay curve, consisting of only four points, into two components of similar half-lives (3 and 1 min).

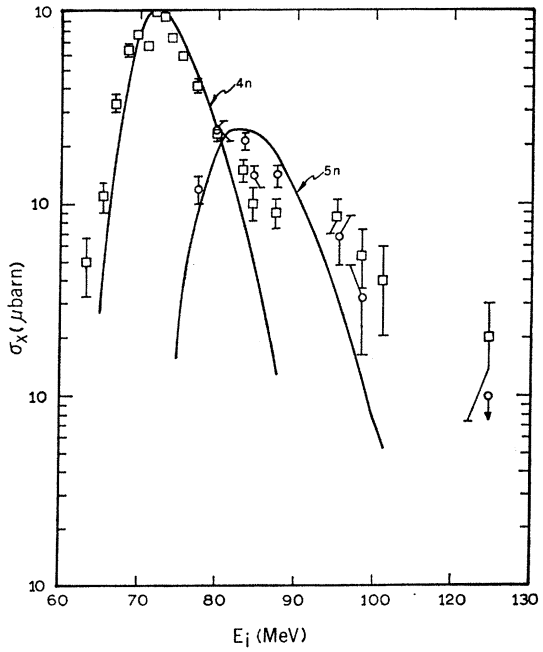

FIG. 4. Experimental cross sections plotted versus ion energy for ^{246}Cm(^{12}C,xn)$^{258-x}$No. The squares and circles correspond to $x=4$ and $x=5$, respectively. The curves represent the function $\sigma_{CN}P_x$ normalized as explained in caption to Fig. 2.

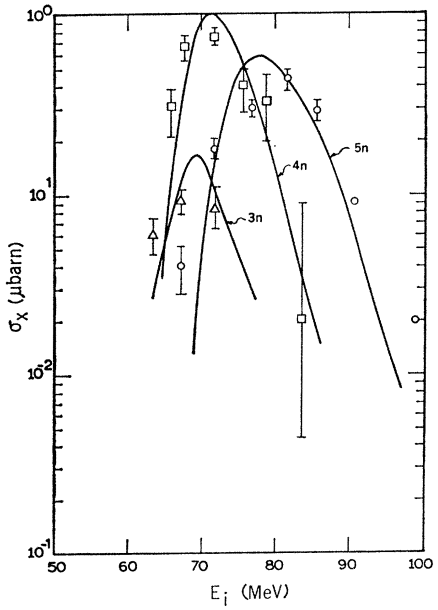

FIG. 6. Experimental cross sections plotted versus ion energy for ^{248}Cm(^{12}C,xn)$^{260-x}$No. The triangles, squares, and circles correspond to $x=3$, $x=4$, and $x=5$, respectively. The curves represent the function $\sigma_{CN}P_x$ normalized as explained in the caption to Fig. 2.

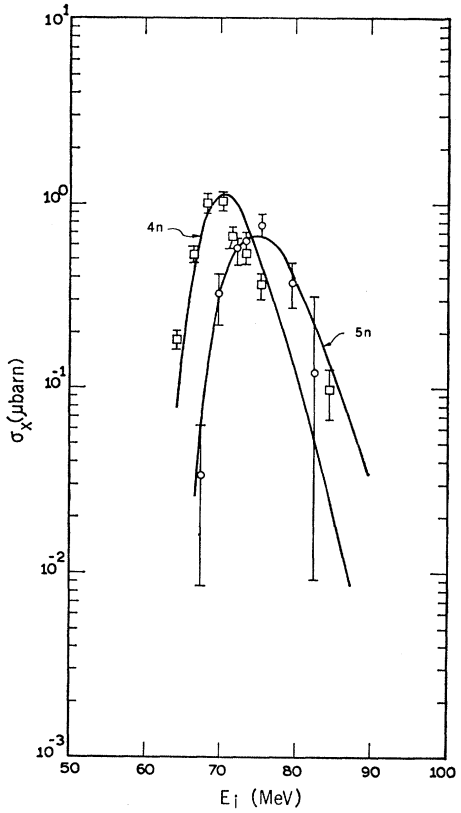

FIG. 7. Experimental cross sections plotted versus ion energy for ^{248}Cm(^{13}C,xn)$^{261-x}$No. The squares and circles correspond to $x=4$ and $x=5$, respectively. The curves represent the function $\sigma_{CN}P_x$ normalized as explained in the caption to Fig. 2.

We notice (see Fig. 2) that, at the highest ion energies, the cross sections for the 2.5-sec SF activity, assigned to ^{252}No, are relatively higher than those for the 8.4-MeV α particles from the same isotope. This may be explained by the presence of SF activity from ^{246}Fm produced in a ^{244}Cm(^{12}C,$\alpha 6n$) reaction. The half-life of ^{246}Fm is 1.5 sec with a SF branching of 8%,[7] and the half-life measurements at the highest energies were not accurate enough to yield a separation of the 2.5- and 1.5-sec components. The assignment of the 2.5-sec SF activity to ^{252}No is first of all based on the fact that its maximum production cross section is at 73 MeV for the system (^{244}Cm+^{12}C) and at 82 MeV for the system (^{244}Cm+^{13}C) (see Figs. 3 and 4).

IV. DISCUSSION

We shall follow closely the procedure used in Ref. 5, in which a good fit to the experimental cross sections was obtained with the following formula:

$$\sigma_x(E_i)=\{\prod_{i=1}^{x}[\Gamma_n/(\Gamma_n+\Gamma_f)]_i\}\sigma_{CN}P_x,$$

where

$$\sigma_{CN}P_x=\sum_{l=0}^{l_{CN}}\sigma_l(E_i)P_{x,l}(E). \quad (1)$$

Here, Γ_n and Γ_f have been defined earlier; E_i is the bombarding energy, σ_l is the cross section for the lth partial wave, l_{CN} is a cutoff value at which the reactions are assumed to change from the compound-nucleus type to the grazing type, and $P_{x,l}(E)$ is the probability for the emission of exactly x neutrons from a compound nucleus of angular momentum l and excitation energy E. Formulas for σ_l, l_{CN}, $P_{x,l}$, and Γ_n/Γ_f shall be given later in the discussion.

Equation (1) is based on the assumption that Γ_n/Γ_f is independent of E_i (or E and l), and thus that the shape of the function is determined by $\sigma_{CN}P_x$. The analysis is therefore performed in two steps. First, we attempt to reproduce the shape of the experimental cross-section curves by adjusting a few parameters in the formula for $P_{x,l}$ (see Sec. IV A). This will give us calculated values for $\sigma_{CN}P_x$. By inserting these values and experimental σ_x values into Eq. (1), we obtain average experimental $\langle\Gamma_n/\Gamma_f\rangle_{av}$ values which will be fitted with calculated ones.

A. Shape of Excitation Function

The values for the quantities σ_l, l_{CN}, and $P_{x,l}$ in the sum term $\sigma_{CN}P_x$ of Eq. (1) are calculated in the following way:

(i) $\sigma_l=\pi\lambda\!\!\!^{-2}(2l+1)T_l$, where $\lambda\!\!\!^{-}$ is the reduced de Broglie wavelength and T_l is the transmission coefficient for the lth partial wave through the following potential $V_l(r)$ between the interacting nuclei[8]:

$$V_l(r)=\frac{Z_1Z_2e^2}{r}+\frac{\hbar^2l(l+1)}{2\mu r^2}+V_0\exp\frac{r_0(A_1^{1/3}+A_2^{1/3})-r}{d}, \quad (2)$$

where Z_i and A_i are their atomic numbers and mass numbers, respectively, $\hbar$ is Planck's constant divided by 2π, μ is the reduced mass of the system, and V_0, r_0, and d are optical-model parameters for which we shall use the empirical values -70 MeV, 1.24 fm, and 0.48 fm, respectively.[9]

We make the approximation that $V_l(r)$ at the peak is parabolic in shape and T_l is then given by[10]

$$T_l=\{1+\exp[2\pi(B-E_c)/\hbar\omega]\}^{-1}.$$

Here, B is the barrier height of $V_l(r)$, E_c is the kinetic energy of both particles in the center-of-mass system, and

$$\omega=[-\partial^2V/\mu\partial r^2]^{1/2},$$

[7] M. J. Nurmia, T. Sikkeland, R. Silva, and A. Ghiorso, Phys. Letters **26B**, 78 (1967).

[8] R. D. Woods and D. S. Saxon, Phys. Rev. **95**, 577 (1954).

[9] V. E. Viola, Jr., and T. Sikkeland, Phys. Rev. **28**, 767 (1962).

[10] D. L. Hill and J. A. Wheeler, Phys. Rev. **89**, 1102 (1952).

where $\partial^2 V/\partial r^2$ is evaluated at the peak of $V_l(r)$, i.e., where $\partial V/\partial r=0$.

(ii) The value of l_{CN} is chosen such that the ratio

$$\sum_{l=0}^{l_{CN}} \sigma_l / \sum_{l=0}^{\infty} \sigma_l$$

(where the sums represent the cross sections for compound-nucleus formation and total interaction, respectively) is equal to the experimental value of 0.8 as obtained for the system ^{238}U+120-MeV ^{12}C.[11] We shall assume the value of this ratio to be independent of E_i.[12]

(iii) $$P_{x,l}(E)=I(\Delta_x,\ 2x-3)-I(\Delta_{x+1},\ 2x-1),$$

where $I(Z,n)$ is Pearson's incomplete Γ function,

$$\Delta_x=(E-\sum_{i=1}^{x} B_i-E_R)/T,$$

and

$$\Delta_{x+1}=(E-\sum_{i=1}^{x} B_i-E_{x+1}{}^f-E_R)/T.$$

Here, E is defined above, B_i is the binding energy of the ith neutron, T is the nuclear temperature, E_R is the rotational energy at the equilibrium configuration and shall be estimated from the formula $E_R=(\hbar^2/2\Im)l(l+1)$, where $\Im$ is the effective moment of inertia, and $E_{x+1}{}^f$ is the fission barrier of the product nucleus ($E_{x+1}{}^f<B_{x+1}$).

The following assumptions are the basis for the estimation of $P_{x,l}$: (1) The nuclear temperature for neutron emission is equal to that for fission and is independent of E and l. (2) The rotational energy at the equilibrium configuration is equal to that at the saddle point. (3) The effective moment of inertia is independent of E and l. (4) Rotational energy is not available for neutron emission and fission.[13] (5) Angular momentum carried off by neutrons is negligible. (6) The angular-momentum distribution does not change during the cascade and is equal to that of the compound nucleus. (7) γ emission takes place only when the excitation energy of a nucleus is less than E_f+E_R.

The calculation of $\sigma_{CN}P_x$, in 2-MeV intervals of E_i, was performed on a CDC 6600 computer. Values for B and E^f were taken from Refs. 14 and 15, respectively; and in the estimation of E we used the masses from Ref. 14. The quantities T and $\hbar^2/2\Im$ were the only adjustable parameters.

Best fit was obtained with $T=1.2\pm0.1$ MeV and $\hbar^2/2\Im=4.5\pm4.5$ keV. These values are identical to those obtained in Ref. 5 for U(C,xn) systems although the errors in $\hbar^2/2\Im$ in the present investigations are larger since only 3, 4, and 5n reactions were involved. We notice that a fit in these cases can actually be obtained with $\hbar^2/2\Im=0$, i.e., with no rotational-energy terms. In Ref. 5, where reactions involving the emission of between 3 and 8n neutrons were analyzed, it was not possible to obtain a fit with $\hbar^2/2\Im=0$. Hence, for comparison we shall in the following adopt the values $T=1.2$ MeV and $\hbar^2/2\Im=4.5$ keV.

The results are shown in Figs. 2–7, where the curves, representing calculated values, are seen to follow the experimental points quite well. The curves are normalized to the experimental points at the peak and are also shifted a certain amount ΔE along the experimental energy scale so as to give the best fit. The values for ΔE for the various systems are given in Table II. The average value of ΔE is 0.2 MeV, with a standard deviation of 1.5 MeV, which is inside the experimental uncertainty of 2 MeV.

The effects of the energy spread of the beam on the width of the excitation functions were not taken into account. Such a correction might make the full width at half-maximum (FWHM) of the peaks as much as 2 MeV smaller.

B. Γ_n/Γ_f Systematics

1. *Experimental* Γ_n/Γ_f *Values*

We define a mean value of Γ_n/Γ_f as

$$\langle\Gamma_n/\Gamma_f\rangle_{av}=\bar{G}/(1-\bar{G}).$$

Here $\bar{G}$ is a mean value of $\Gamma_n/(\Gamma_n+\Gamma_f)$ defined as

$$\bar{G}=\{\prod_{i=1}^{x}[\Gamma_n/(\Gamma_n+\Gamma_f)]_i\}^{1/x}$$

that, according to Eq. (1), is given by

$$\bar{G}=[\sigma_x/(\sigma_{CN}P_x)]^{1/x}. \tag{3}$$

Values for $\langle\Gamma_n/\Gamma_f\rangle_{av}$, estimated at the peak of σ_x and $\sigma_{CN}P_x$, are listed in Table II together with the quantity A_{av} which represents the mass number of the intermediate fissioning nucleus half-way along the evaporation chain. The errors for $\langle\Gamma_n/\Gamma_f\rangle_{av}$ are about 50, 25, and 20% when $\langle\Gamma_n/\Gamma_f\rangle_{av}$ is estimated from a 3n, 4n, and 5n reaction, respectively. They include experimental errors in σ_x and uncertainties in $\sigma_{CN}P_x$ due to uncertainties of 0.02 fm in r_0 and d, 0.1 MeV in T, and 4.5 keV in $\hbar^2/2\Im$.

2. *Semiempirical Formula for* $\langle\Gamma_n/\Gamma_f\rangle_{av}$

We have assumed above that Γ_n/Γ_f is independent of both E and l. A formula for Γ_n/Γ_f that does not contain E or l was developed by Fujimoto and Yamaguchi.[4] Using this formula and including odd-even terms,[13] the

[11] T. Sikkeland, and V. E. Viola, Jr., in *Proceedings of the Third Conference on Reactions Between Complex Nuclei, Asilomar, 1963,* edited by A. Ghiorso, R. M. Diamond, and H. E. Conzett (University of California Press, Berkeley, 1963).
[12] T. Sikkeland, Phys. Rev. **135**, B669 (1964).
[13] J. R. Huizenga and R. Vandenbosch, in *Nuclear Reactions,* edited by P. M. Endt and P. B. Smith (North-Holland Publishing Co., Amsterdam, 1962).
[14] V. E. Viola, Jr., and G. T. Seaborg, J. Inorg. Nucl. Chem. **28**, 698 (1966).
[15] V. E. Viola, Jr., and B. D. Wilkins, Nucl. Phys. **82**, 65 (1966).

TABLE II. Results of the analysis of experimental excitation functions for Cm(C,xn)No reactions. Here, $\sigma_{x,m}$ represents the maximum cross section and $E_{i,m}$ the corresponding ion energy in the laboratory system, as read off the curves in Figs. 2–7; ΔE gives the amount we have shifted the calculated curves in the figures along the experimental energy scale to obtain a fit; $(\sigma_{CN}P_x)_m$ is the calculated maximum cross section for a (C,xn) reaction when fission competition is ignored; A_{av} represents the mass number of the intermediate fissioning nucleus half-way along the evaporation chain. In the last three columns of the table, experimental $\langle\Gamma_n/\Gamma_f\rangle_{av}$ values are compared with values calculated from Eq. (4) and with those obtained from Eq. (5).

System	x	$E_{i,m}$ (MeV)	ΔE (MeV)	$\sigma_{x,m}$ (μb)	$(\sigma_{CN}P_x)_m$ (mb)	A_{av}	$\langle\Gamma_n/\Gamma_f\rangle_{av}$ (expt)	Eq. (4)	$\langle\Gamma_n/\Gamma_f\rangle_{av}$ Eq. (5)
^{244}Cm+^{12}C	4	73.3	0	0.25[a]	90	254.5	0.054	0.039	0.043
	5	83.0	−2	0.090	330	254	0.051	0.033	0.037
^{244}Cm+^{13}C	3	69.8	0	0.12	0.8	256	0.056	0.063	0.060
	4	72.8	0	0.30	77	255.5	0.046	0.052	0.054
	5	82.0	−2	0.16[a]	250	255	0.061	0.053	0.047
^{246}Cm+^{12}C	4	72.0	0	1.0	50	256.5	0.072	0.063	0.064
	5	83.0	−3	0.24	290	256	0.065	0.053	0.058
^{246}Cm+^{13}C	3	67.5	2	0.07	0.60	258	0.051	0.083	0.076
	4	69.5	2	0.62	43	257.5	0.065	0.071	0.072
	5	78.5	2	0.56	430	257	0.071	0.071	0.068
^{248}Cm+^{12}C	3	69.2	0	0.16	0.70	259	0.065	0.073	0.085
	4	71.2	0	1.0	26	258.5	0.085	0.076	0.080
	5	77.8	0	0.58	240	258	0.081	0.069	0.076
^{248}Cm+^{13}C	4	70.5	1	1.1	30	259.5	0.084	0.087	0.090
	5	74.8	1	0.66	150	259	0.093	0.081	0.085

[a] The combined cross sections for the 2.5-sec, 8.4-MeV α emitter and the 2.5-sec SF emitter.

geometric mean value for Γ_n/Γ_f in a cascade of x neutrons from an even-Z nucleus can be written as[5]

$$\langle\Gamma_n/\Gamma_f\rangle_{av}=cA_{av}^{2/3}\exp(\beta\Delta/x)\times\exp\{[\sum_{i=1}^{x}(E_i^f-B_i)]/xT\}, \quad (4)$$

where A_{av}, E_i^f, B_i, and T have been defined earlier, c and Δ are constants, and

$$\begin{aligned}\beta&=\ 0, \quad n_{ee}=n_{eo}\\ &=\ 1, \quad n_{ee}>n_{eo}\\ &=-1, \quad n_{ee}<n_{eo}.\end{aligned}$$

(n_{ee} and n_{eo} are the numbers of even-even and even-odd nuclides in the cascade, respectively.) This formula, which is a good approximation for $E-B_i\geqq 3$ MeV,[13] is based on the constant-temperature level-density formula[13] (as is the formula for $P_{x,l}$) and on the assumption that pairing energies only depend on the even or odd characters of Z and N.

Values for $\langle\Gamma_n/\Gamma_f\rangle_{av}$ calculated according to this formula were now fitted to the experimental ones by adjusting the constants c, Δ, and T, and using the values for B and E^f from Refs. 14 and 15, respectively. Best fit was obtained with $c=0.63$, $\Delta=1.4$, and $T=0.6$ MeV, which reproduced the experimental values with a standard deviation of 22%. Calculated $\langle\Gamma_n/\Gamma_f\rangle_{av}$ values are compared to the experimental ones in Table II.

When only $4n$ and $5n$ cross sections are considered, the experimental values are reproduced with a standard deviation of 10%. This is a factor of 2 better than the estimated experimental errors. The reason for this is that the calculated values are normalized to the experimental ones and hence systematic experimental errors are eliminated.

A closer examination of the experimental and calculated $\langle\Gamma_n/\Gamma_f\rangle_{av}$ values in Table II reveals that, for $3n$ reactions, the former are systematically and on the average 30% lower than the latter. This discrepancy can be removed by using a value of 1.1 MeV instead of 1.2 MeV for the nuclear temperature in the estimation of $\sigma_{CN}P_x$. This will increase the experimental $\langle\Gamma_n/\Gamma_f\rangle_{av}$ values for the $3n$ reactions by 30%, whereas those for the $4n$ and $5n$ reactions are practically unchanged. The values of the other parameters r_0, d, V_0, and $\hbar^2/2\Im$ have little influence on the relative values of $\langle\Gamma_n/\Gamma_f\rangle_{av}$. We may therefore conclude that Γ_n/Γ_f, within experimental errors, is independent of bombarding energy. This is in agreement with the conclusion drawn in Ref. 5 on the basis of a similar analysis of reactions involving the emission of between 3 and 8 neutrons.

The values for c, Δ, and T obtained in Ref. 5, where $\langle\Gamma_n/\Gamma_f\rangle_{av}$ for Cf isotopes were analyzed, were 0.33, 1.5, and 0.59 MeV, respectively. The large difference between the c values from these two sets of experiments is significant. This disparity is regarded as outside experimental errors. Rather, we think it is in large part due to uncertainties in the values of E^f used. We find a value of 0.5 for c if we assume that the E^f values for the Cf isotopes are systematically 0.2 MeV too high and those for No isotopes 0.2 MeV too low. By extending these calculations to lighter actinides the discrepancies became even larger. For instance, to obtain a fit to experimental Γ_n/Γ_f values for uranium isotopes, the E^f values from Ref. 15 have to be decreased by about 0.8 MeV. This suggests either some systematic and primarily Z-dependent deviations in these values or a breakdown of Eq. (4).

3. *Empirical Formula for* Γ_n/Γ_f

The systematic variation of Γ_n/Γ_f with N is illustrated in Fig. 8 for trans-berkelium nuclei of even Z.

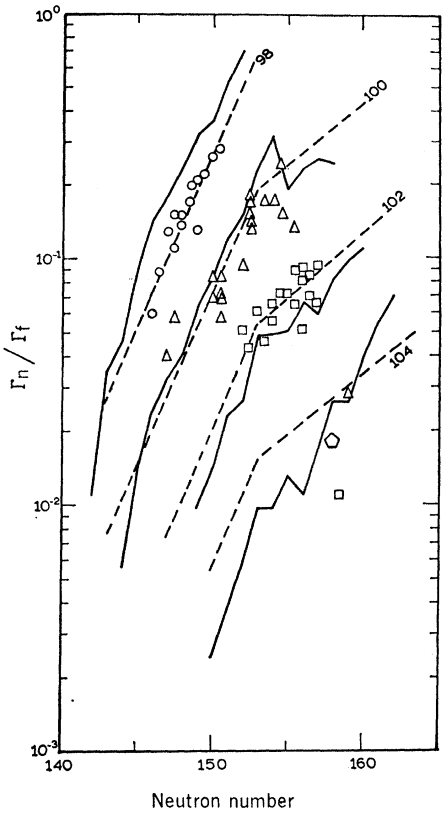

FIG. 8. Experimental Γ_n/Γ_f values for even-Z trans-berkelium nuclides plotted versus the neutron number of the intermediate nucleus in the neutron cascade. The data are from the present work, from Ref. 5, and from Ref. 17. The circles, triangles, and squares represent data for Cf, Fm, and No, respectively. For element 104 we have indicated three possible values for $\langle\Gamma_n/\Gamma_f\rangle_{av}$ based on the assumptions that the SF emitter observed (see Ref. 18) in the reaction between ^{242}Pu and ^{22}Ne is produced in a $3n$ (triangle), $4n$ (square), and $5n$ (pentagon) reaction, respectively. The solid lines connect individual Γ_n/Γ_f values calculated from Eq. (4) as explained in the text; and the broken lines represent the empirical relationship of Eq. (5).

Here the points represent experimental $\langle\Gamma_n/\Gamma_f\rangle_{av}$ values and the solid and broken lines that connect individual Γ_n/Γ_f values for nuclides of the same element represent, respectively, Eq. (3), with $x=1$, $c=0.5$, $T=0.59$ MeV, and $\Delta=1.5$, and the following empirical equation:

$$\log_{10}(\Gamma_n/\Gamma_f)=-0.276Z+\begin{cases}5.46+0.140N, & \text{for } N\leqq 153\\ 19.23+0.050N, & \text{for } N\geqq 153.\end{cases} \quad (5)$$

We see that the empirical equation gives a better overall fit. In fact, we find that Eq. (5) reproduces well all the experimental Γ_n/Γ_f values for even-Z trans-thorium nuclides. [A similar good fit for odd-Z nuclides is obtained by adding 0.12 to the right side of Eq. (5).] Hence, such a formula is more realistic to use in cross-section calculations in the vicinity of nuclei for which Γ_n/Γ_f values are known.

This very nearly linear relationship between $\log(\Gamma_n/\Gamma_f)$ and N, or A, below the $N=152$ subshell has been pointed out by several authors.[13] It is interesting to note that the data from the No isotopes presented here suggest a similar but less steep relationship above that shell. Such a trend is also reproduced by Eq. (4) in conjunction with E^f and B values from Refs. 14 and 15.

Using Eq. (4) in conjunction with Cameron's values for B and his shell and pairing corrections[16] for the estimation of E^f, it was predicted in Ref. 17 that $\log(\Gamma_n/\Gamma_f)$ in the region of the 152 shell is almost symmetric with respect to $N=153$, i.e., that $\log(\Gamma_n/\Gamma_f)$ decreases almost as fast with N above $N=153$ as it increases with N below that neutron number. The fit to experimental data was good below $N=153$. This suggests, therefore, that above $N=153$, Cameron's values do not reproduce the systematic trend as well as do those from Refs. 14 and 15.

The three experimental points given for element 104 represent $\langle\Gamma_n/\Gamma_f\rangle_{av}$ values estimated from the experimental cross section[18] for the production of a 0.3-sec SF emitter in the reaction between ^{242}Pu and ^{22}Ne, assuming a $3n$, $4n$, and $5n$ reaction, respectively. Comparison with the extrapolated Γ_n/Γ_f values using both Eqs. (4) and (5) suggests the $3n$ and $5n$ reactions to be the most likely candidates. In the latter case this emitter is ^{259}104, which also should be produced in a ^{242}Pu(^{20}Ne,$3n$) reaction. Since this was shown experimentally not to be the case,[16] one may conclude that this activity is more likely due to ^{261}104, rather than ^{260}104 as implied in Ref. 16. However, the Γ_n/Γ_f systematics are, of course, too uncertain to make this isotope assignment definite.

V. CONCLUSION

The shapes of the experimental excitation functions are successfully reproduced by the calculated curves and such curves can therefore be used in mass assignments. To predict values of the absolute cross sections it appears, at the present time, more realistic to use an empirical formula for Γ_n/Γ_f, such as Eq. (5). In using the Fujimoto-Yamaguchi formula [Eq. (4)] one has to rely on rather questionable values for the fission barrier and the neutron binding energy. Here an uncertainty of only 0.2 MeV in the quantity E_f-B_n will introduce an error of about 40% in the value of Γ_n/Γ_f. This error corresponds to an uncertainty of a factor of 3 in the predicted value for a $4n$ cross section in a region where Γ_n/Γ_f is about 0.1. One might therefore suggest a reverse procedure, namely, to use Eq. (4) in conjunction with experimental $\langle\Gamma_n/\Gamma_f\rangle_{av}$ values to obtain "experimental" values for E_f-B_n.

[16] A. G. W. Cameron, Can. J. Phys. **35**, 1021 (1957).
[17] T. Sikkeland, Lawrence Radiation Laboratory Report No. UCRL-16348, 1965 (unpublished).
[18] G. N. Flerov *et al.*, At. Energ. (USSR) **17**, 310 (1964) [English transl.: Soviet J. At. Energy **17**, 1046 (1964)].